ISSN: 0973-4929, Vol. 21, No. (1) 2026, Pg. 266-286

Current World Environment

www.cwejournal.org

Modelling Land Use Dynamics and Urban Growth Analysis using Random Forest Model and Shannon Entropy-Based Approach in Bidhannagar Municipal Corporation, West Bengal, India

VAJANA MONDAL, YAMANUR VENKATA KRISHNAIAH*, MOUMITA HATI, DEBASIS DAS, MANIKA MALLICK, KAUSIK PANJA, DEEPA RAI, and ATOSHI CHAKMA

Department of Geography and Disaster Management, Tripura University (A Central University), Suryamaninagar, Tripura, India.

Abstract

In India, urbanisation has been a significant phenomenon, driving population growth and city expansion. It plays a crucial role in shaping the Earth's surface. Hence, this paper aims to analyse land-use patterns and change detection, and to determine urban growth in the Bidhannagar area. Bidhannagar has developed as a planned satellite town to address the growing population of Kolkata for the housing demand. This study uses satellite images to analyse the spatial and temporal dynamics of LULC changes. Landsat 5 Thematic Mapper for 2001 and 2011, and Landsat 8 Operational Land Imager for 2021 and 2024 have been used for LULC classification. Further, the Random Forest Model was applied in Google Earth Engine to analyse LULC patterns for selected years, and also worked out urban growth using the Urban Expansion Area Intensity Index (UAEII), Shannon Entropy model, and the Landscape Expansion Index (LEI). The results showed a significant decline in wetlands from 25.88% to 20.70%, green spaces from 21.25% to 16.89%, fallow land from 13.66% to 9.45%, and water bodies from 5.48% to 2.79% from 2001 to 2024, while the built-up area grew substantially from 33.72% to 50.17%. The Kappa Coefficient was applied to assess accuracy of image classification that are 0.81, 0.84, 0.86, and 0.89 for the years 2001, 2011, 2021, and 2024, respectively. UAEII from 2001 to 2024 indicates that the built-up

Article History
Received: 23 February 2026
Accepted: 28 April 2026

Keywords
Bidhannagar Municipal Corporation;
Land use dynamics;
Random Forest (RF);
Shannon Entropy;
Urban Growth;
Urban Expansion Area Intensity Index (UAEII).

CONTACT Yamanur Venkata Krishnaiah yvkrishna09@gmail.com Department of Geography and Disaster Management, Tripura University (A Central University), Suryamaninagar, Tripura, India.

Doi: http://dx.doi.org/10.12944/CWE.21.1.19

area is increasing at a moderately and Shannon Entropy reflects urban growth in a compact manner in the NE, SE, and SW zones, while LEI emphasises the pattern of the built-up area's expansion. This paper offers valuable insights for developing more comprehensive and strategic land-use policies and management approaches in this study area.

Introduction

Land-use change is essential for understanding the relationship between nature and humans.[1] Land use describes how humans utilise land resources for various needs, while land cover shows the physical characteristics of the Earth's surface.[2,3] In recent decades, rapid urbanisation has accelerated global land use changes.[4,5] Converting vegetation and agricultural land to built-up, impervious surfaces has increased, especially in urban areas.[6] The expansion fragments natural habitats, depletes ecosystem services, and affects urban stability. It impacts socioeconomic conditions, biodiversity, climate, and reshapes the environmental status.[7] Understanding the detection of LULC change is vital for management of resources, urban planning, and sustainability.[8-13]

Bidhannagar, a satellite town of Kolkata, is known for its organised layout, extensive roads, and green spaces, but is transforming into a commercial and IT hub, affecting land use and urban growth. Previous studies mainly focused on spatiotemporal changes in LULC, and a comparative study of Salt Lake and New Town was also conducted, in which LULC and the air quality index were analysed.[14,15] The amalgamation of Rajarhat-Gopalpur Municipality and Mahishbathan II Gram Panchayat, Bidhannagar Municipal Corporation underwent major administrative and spatial restructuring. However, no recent comprehensive study has examined post-organisation LULC dynamics together with quantitative measures of urban growth in the BMC area. Existing studies have lacked integration of LULC transformation with quantitative measures of urban expansion, such as application of RF in Google Earth Engine, Shannon entropy,[16-18] Urban Area Expansion Intensity Index (UAEII), and Landscape Expansion Index (LEI).[19-22] Therefore, there is a need to analyse LULC dynamics and urban growth together using an integrated remote sensing and GIS-based approach.

The present study highlights advanced remote sensing and modelling techniques to analyse patterns and changes in LULC. Moderate-resolution satellite imagery and classification algorithms were used to categorise the study area. This research aims to examine (a) land use land cover patterns analysis. (b) transition of LULC categories from one class to another, and (c) urban growth explanation using UAEII, Shannon entropy and LEI in Bidhannagar Municipal Corporation.[23-25] Bidhannagar is developing to accommodate Kolkata's growing population. Therefore, this analysis guides resource management, sustainable development strategies, and the achievement of long-term development goals.

Materials and Methods

Study Area

Bidhannagar Municipal Corporation is located on the eastern side of Kolkata City, and its latitude and longitude range from 22°31′30″ to 22°40′02″ N and 88°23′45″ to 88°28′29″ E, respectively. The study region covers an area of about 57.26 km². The total population of Bidhannagar Municipal Corporation is approximately 6.15 lakh, with a population density of 1030 persons per sq.km (2011 census). In 1991, Bidhannagar Municipality was established. After merging the Rajarhat Gopalpur Municipality and the Mahishbathan II Gram Panchayat, the Bidhannagar Municipal Corporation (BMC) was formed to enhance urban planning and management of Salt Lake and Rajarhat with total wards no. 41. The study area borders Madhyamgram and North Dumdum Municipalities to the north, Rajarhat Block to the south, South Dumdum Municipality to the west, and HIDCO New Town to the east (Fig. 1). Bidhannagar Municipal Corporation features a diverse layout, with Salt Lake City displaying a grid structure divided into five sectors. Sectors I-IV are mainly residential and commercial, while Sector V includes commercial and IT hubs, and it was previously NDITA (Nabadiganta

Industrial Township Authority). NDITA was separated from Bidhannagar in 2006 and developed a new township. The study covers these four sectors plus NDITA. Bidhannagar connects via VIP road, Eastern Metropolitan Bypass, and East-West Metro, IT, residential, commercial centres, and transport infrastructure, shaping its vibrant urban landscape and land-use patterns.

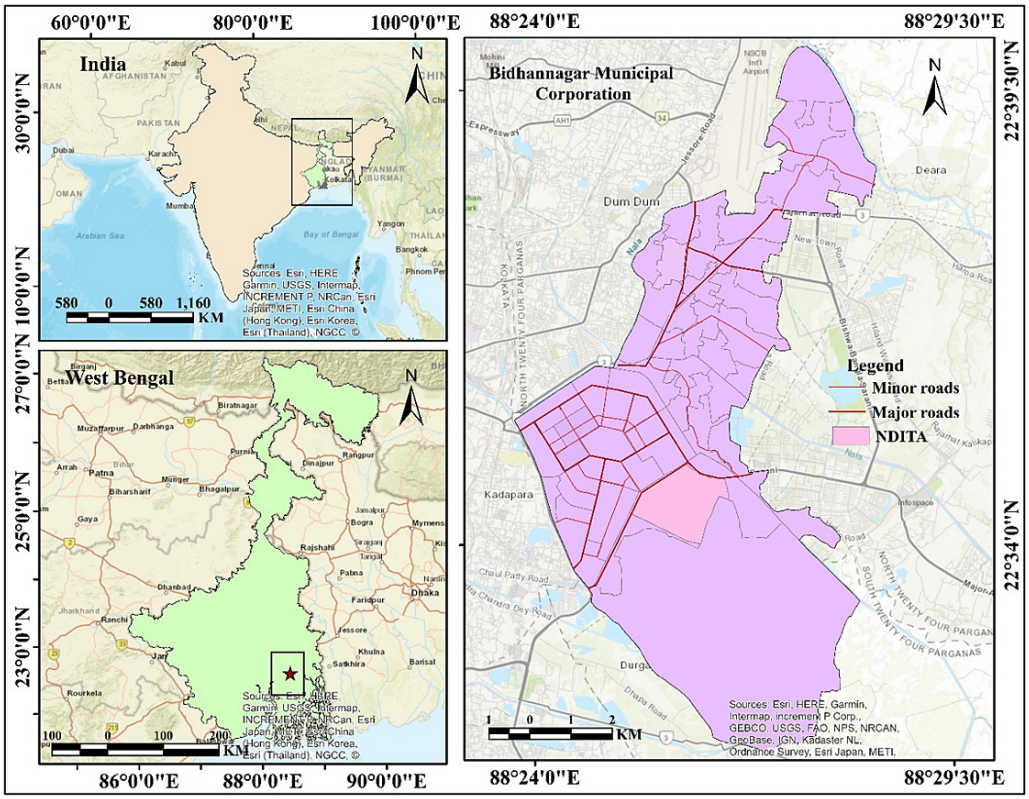

Fig.1: Location Map of the Study Area

Dataset Acquisition and Image Pre-Processing

Landsat 5 Thematic Mapper for 2001 and 2011, and Landsat 8 Operational Land Imager for 2021 and 2024, were downloaded from the USGS open-source website to understand past and present land-use patterns (Fig. 2 & Table 1). For selected years, annual composite images have been generated for LULC classification using composite condition elements, including filterDate to specify the required date range for obtaining the maximum land surface details, filterBounds to delimit the study area boundary, and finally, a median reducer function to obtain the composite image collection. It ensures temporal consistency and reduces annual variability in spectral reflectance while minimising the influence of seasonal dynamics, such as dry and wet conditions. This approach enables a more accurate delineation of the actual land-use classification within the study area, thereby eliminating seasonal bias. Preprocessing satellite imagery is an important step in remote sensing analysis to ensure the accuracy of outcomes.[26] The cloud-mask process is applied to improve image quality and accurately detect surface features. The quality assessment band is used to remove cloud-contaminated pixels, and cloud-free imagery is produced using a median composite approach. The atmospheric and radiometric corrections are also done to protect the datasets from atmospheric disturbances and sensor distortions using the Landsat Ecosystem Disturbance Adaptive Processing System (LEDAPS) and Landsat Surface Reflectance Code (LaSRC) in Google Earth Engine (GEE).[27,28] Further, layer stacking has been executed to composite the multiple spectral bands which served the primary input for LULC classification and urban growth analysis, and median

values have been used to minimise the impact of outliers, improve classification stability, and provide a more representative dataset for training.[29] The multiple spectral bands include Blue, Green, Red, Near-Infrared (NIR), and Shortwave Infrared (SWIR) would help to categorise the LULC patterns.

Table 1: Satellite Imagery and Acquisition Details

Satellite Image	Acquisition year	Sensor	Resolution (m)	Bands	GEE Products
Landsat 5	2001, 2011	Thematic Mapper (TM)	30	B1, B2, B3, B4, B5	Landsat/LT05/C02/T1_L2
Landsat 8	2021, 2024	Operational Land Imager (OLI)	30	B1, B2, B3, B4, B5, B6, B7	Landsat/LC08/C02/T1_L2

Source: USGS

Image Classification Using Random Forest (RF) Model in Gee

Image classification was performed using the Random Forest Model, a supervised machine learning algorithm, in GEE, a cloud-based platform, to identify land use patterns for 2001, 2011, 2021, and 2024. The RF model is widely used for its ability to manage huge datasets, robustness, and high accuracy.[30] This model is a non-parametric ensemble learning algorithm that employs hyperparameter tuning to reduce overfitting.[31-33] The RF model is trained with classified data and subsequently tested for accuracy. The number of trees (ntree) has been set to 150 via hyper-tuning to improve classification accuracy. The training process begins with collecting training samples for each LULC category using a supervised image classification technique. These samples are generated from real-world observations and historical land-use records. In the BMC area, five LULC categories were identified: built-up, wetlands, green spaces, fallow land, and water bodies. The land use categories were identified based on satellite imagery reflectance values, and a primary survey was conducted to obtain field observations for distinguishing the different LULC categories. Within these categories, built-up areas include residential, commercial, and industrial zones. Wetlands cover parts of the East Kolkata Wetland, a designated Ramsar site, while the water bodies include ponds and canals. Urban green space comprises recreational areas such as parks and gardens, as well as vegetation along streets and road dividers. Fallow lands are cultivable wastelands and marshy regions. For this study, total 220 training samples were collected from each year to classify the study area. After collecting the samples, the dataset was separated into training and testing subsets. Across the LULC map of the study area, 200 ground control points were generated through stratified random sampling to ensure balanced distribution across the classified categories for each selected year, and a confusion matrix was prepared. Separate training samples were collected for each year, and the independent RF model was trained. Of the total samples, 70% were used for training and 30% for testing, ensuring the model's learning and validation. These datasets facilitate the development of the classification model and its accuracy assessment.[34]

Accuracy Assessment

Accuracy assessment evaluates the reliability of LULC classification. Using 30% of the dataset, split during preparation for unbiased evaluation, it compares classified outputs with reference data to calculate metrics such as overall accuracy, producer's and user's accuracy, and the Kappa coefficient. User's accuracy shows the percentage of correctly classified pixels in a LULC category, while producer's accuracy assesses captures ground-truth features.[35] A confusion matrix was used to determine these accuracies, with overall accuracy and the Kappa coefficient evaluating overall performance across years. The formulas used to compute these values are included.

$$Producer's\ accuracy\ (UA) = \left(\frac{S_{XX}}{S_{X+}}\right) \times 100 \quad ...(1)$$

$$User's\ accuracy\ (PA) = \left(\frac{S_{XX}}{S_{+X}}\right) \times 100 \quad ...(2)$$

$$Overall\ Accuracy = \frac{1}{N}\sum_{k=1} n_i \times 100 \quad ...(3)$$

$$Kappa\ Coefficient = \frac{N\sum_{i=1}^{r} S_{XX} - \sum_{i=1}^{r}(S_{X+}.S_{+X})}{N^2 - \sum_{k=1}^{r}(S_{X+}.S_{+X})} \quad ...(4)$$

Where S_{XX} is the diagonal element; S_{X+} and S_{+X} is the total items in the row and column X*r* is the number of rows and columns of the confusion matrix, and N denotes the number of observations. User's, Producer's, and Overall accuracy range from 0 to 100%, and the Kappa coefficient indicates the value between 0 and 1.[36]

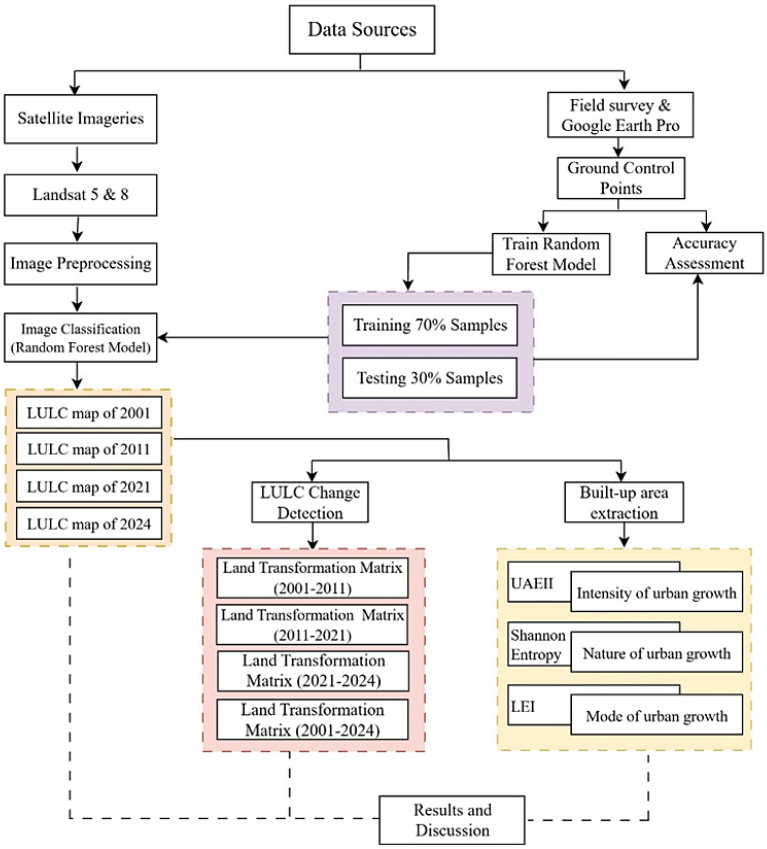

Fig.2: Methodological Flow Chart for LULC and Urban Growth

Spatio-Temporal Land use Change Detection (Land Transformation Matrix)

Spatiotemporal change detection, or land transition, helps determine how LULC patterns change from one land type to another.[37] The land transformation matrix was prepared to provide an overview of LULC transformation.[5] The matrix has been calculated using the following formula:

$$T_{ij} = \begin{bmatrix} T_{11} & T_{12} & : & T_{1n} \\ T_{21} & T_{22} & : & T_{2n} \\ : & : & : & : \\ T_{n1} & T_{n2} & : & T_{nn} \end{bmatrix} \quad ...(5)$$

Where T_{ij} indicates the land area transformation from LULC class i in the previous year and LULC class j in the next year. This matrix can easily identify the

major LULC transformation, and the transformation map represents the area in the study region that is transitioning.

Measurement of Urban Expansion Using Urban Area Expansion Intensity Index (UAEII)

An UAEII is a quantitative index that assesses the rate and intensity of built-up expansion over a specified timeframe.[38,39] This index analyses the spatial-temporal dynamics of urban expansion. It helps evaluate the extent of urban built-up and identify areas of concentrated urban growth.[40] An UAEII has been calculated using the following equation:

$$UAEII = \frac{BU_{t2} - BU_{t1}}{TA \times (t_2 - t_1)} \times 100 \quad ...(6)$$

In this equation, BU_{t2}= present year built-up extent, BU_{t1}= initial year built-up extent, TA=Total area of the study region and ($t_2 - t_1$)= Difference of time between the present and the initial year. The UAEII is divided into five distinct classes based on its numerical range, which spans from 0 to values exceeding 1.92. A UAEII value range from 0 to 0.28 reflects slow development. A value between 0.28 to 0.59 signifies low-speed urban expansion. Values from 0.59 to 1.05 correspond to medium-speed growth, whereas a UAEII between 1.05 and 1.92 indicates high-speed development. If the UAEII value surpasses 1.92, it is classified as very high-speed urban expansion, reflecting rapid and intense urbanisation.41 This classification provides a standardised framework for assessing urban growth dynamics and for monitoring the magnitude of urban expansion over time.

Shannon Entropy for Assessing Urban Growth

Shannon entropy is an indicator of urban diversity.42 Shannon entropy was first introduced in the 1948 paper "A Mathematical Theory of Communication" by Claude Shannon.[24] It is a widely used approach for assessing the concentration and spatial distribution of urban growth.[43] The entropy is essential for understanding the dynamics of urban sprawl.[44] It enables the assessment of concentrated or scattered growth, offering valuable insights into the dynamics of urban expansion.[45] Using the following equation, Shannon entropy has been expressed

$$H_n = -\sum_{i=1}^{n} P_i \,.\, log_e(P_i) \quad ...(7)$$

Where H_n = Shannon entropy, P_i = The built-up shares in the buffer zone *i* , *n* = total buffer zones. The Shannon entropy value range is from 0 to log(n). The entropy value nearest to zero indicates compact urban growth. Whereas the value is close to log(n) suggests scattered, segmented urban growth.[46]

Relative entropy is also a robust quantitative measure for identifying changes in urban land use by comparing past and present spatial configurations. The entropy is calculated using the formula[47]:

$$H'_n = \frac{H_n}{log_e(n)} \quad ...(8)$$

Relative entropy has been used to normalise Shannon's entropy to a scale ranging from 0 to 1.[48] The value of relative entropy 0 represents the compact and aggregated built-up pattern, and 1 represents a discrete built-up distribution. The midpoint is set as the threshold value, and values above it (0.5) indicate urban sprawl.[49]

Landscape Expansion Index (LEI)

The landscape expansion index is a spatial metric that analyses urban growth by classifying new land patches based on their relationship to existing built-up areas.[50] It identifies growth modes: infilling, where growth occurs within existing areas; edge expansion, which develops outward from boundaries; and leapfrog development, where areas are isolated from existing ones. The LEI have been extracted based on the following formula[51]:

$$LEI = \frac{A_p}{A_p + A_n} \times 100 \quad ...(9)$$

Where A_p indicates the number of new pixels adjacent to pre-existing pixels of built-up, while A_n denotes the new urban pixel number isolated from pre-existing urban areas. A LEI of 0 indicates outlying or leapfrog development, with new patches disconnected from

existing areas. Values between 0 and 50 indicate edge expansion, a mix of isolated and adjacent growth. Above 50 signifies infilling, with new urban pixels mostly within or near developed zones, increasing density.[52]

Results

LULC Pattern Analysis

The LULC patterns offer a comprehensive view of the landscape's spatial and temporal changes. The selected study area is categorised as five distinct LULC types: built-up area, wetland, green space, fallow land, and water bodies. According to the 2001 LULC classification, built-up area dominated, its occupying nearly 19.31 km² (33.72%) of the total area. The southern and southeastern parts of BMC showed wetlands covers 25.88%, while green spaces account was 21.25%, followed by smaller portion covered by fallow land (13.66%) and water bodies (5.48%) (Fig. 3, 4a & Table 2). By 2011, the built-up area increased up to 39.35%, mainly in the central region, including Sectors I, II, III, IV, and V, which attract many residents due to the presence of administrative buildings and IT hubs. During this period, wetland (24.59%), green space (20.38%), fallow land (11.79%), and water bodies (3.89%) experiences continuous decline (Fig. 3, 4b & Table 2). The LULC map of 2021 shows the built-up areas occupy the largest region (45.46%) mainly in the core and outskirts of the study region, while wetland (22.56%), greenspace (17.92%), fallow land (11.11%), and waterbodies (2.95%) continuously decreased (Fig. 3, 4c & Table 2). For the year 2024 highlighted that built-up area increased up to 50.17%, while wetland, green space, fallow land, and waterbody areas decreased in BMC. From 2001 to 2024, the total built-up area was increased, remains categories drastically decreased.

Table 2: Temporal Distribution of LULC Classes (2001 to 2024)

LULC Categories/ Classes	2001		2011		2021		2024	
	Area (km²)	Area (%)	Area (km²)	Area (%)	Area (km²)	Area (%)	Area (km²)	Area (%)
Built-up	19.31	33.72	22.53	39.35	26.03	45.46	28.73	50.17
Wetland	14.82	25.88	14.08	24.59	12.92	22.56	11.85	20.70
Greenspace	12.17	21.25	11.67	20.38	10.26	17.92	9.67	16.89
Fallow land	7.82	13.66	6.75	11.79	6.36	11.11	5.41	9.45
Waterbodies	3.14	5.48	2.23	3.89	1.69	2.95	1.60	2.79

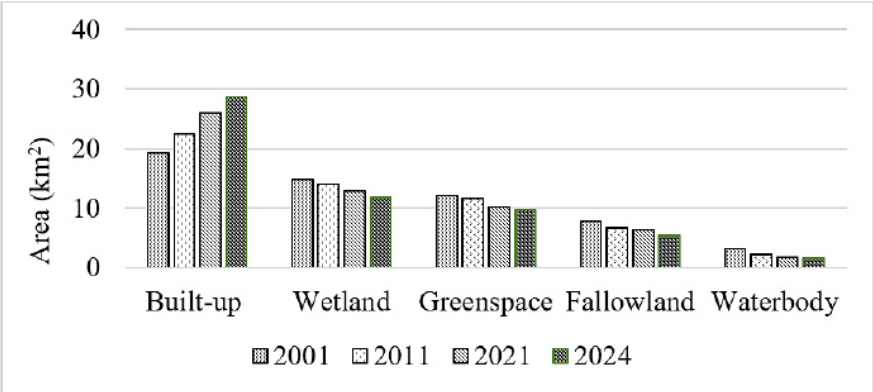

Fig. 3: Temporal Distribution of LULC Categories from 2001 to 2024

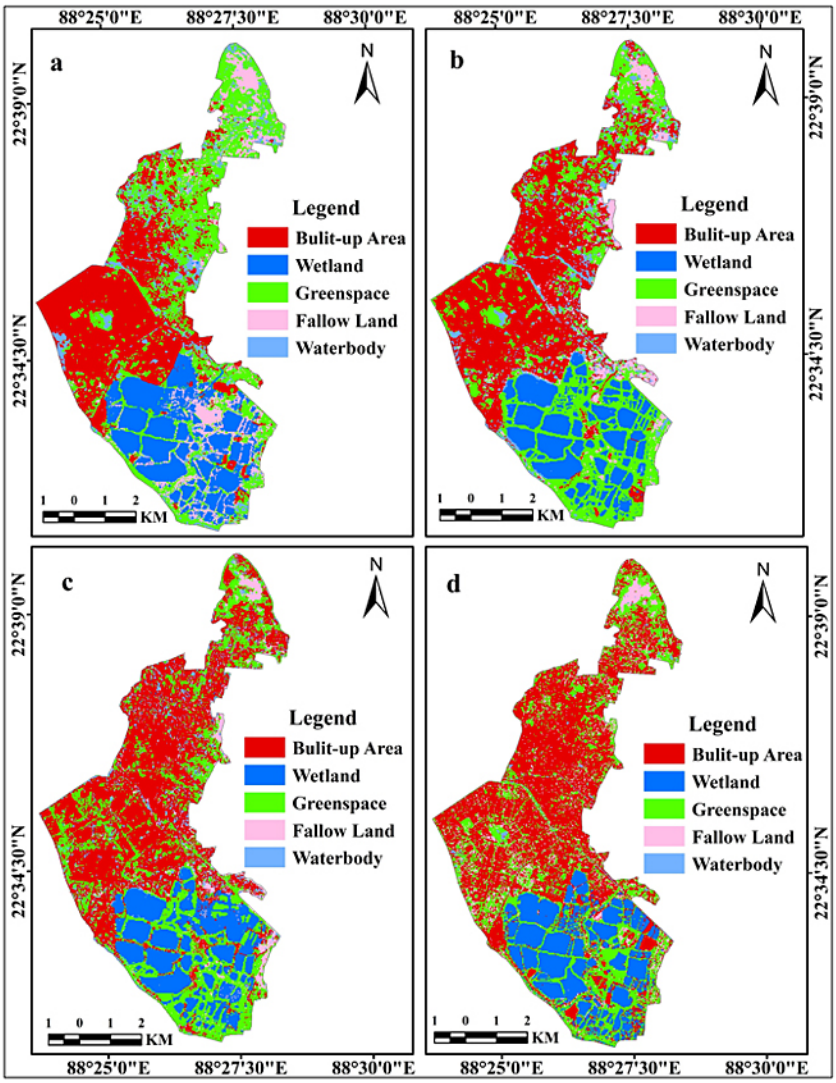

Fig. 4: Spatio-temporal Distribution of Land Use Land Cover Map (a. 2001, b. 2011, c. 2021, d.2024)

Table 3: Assessment of Accuracy of LULC of BMC (2001 to 2024)

LULC Class	2001		2011		2021		2024	
	UA	PA	UA	PA	UA	PA	UA	PA
Built-up Area	81.63	80.00	90.91	89.29	94.64	86.89	94.64	89.83
Wetland	89.83	88.33	90.48	90.48	92.73	92.73	91.94	95.00
Greenspace	85.71	84.00	91.11	87.23	89.36	89.36	95.25	93.18
Fallow land	91.30	87.50	78.95	88.24	77.78	87.50	78.95	88.24
Waterbody	75.00	93.75	77.78	82.35	75.00	85.71	87.50	87.50
Overall Accuracy	85.50		88.50		89.00		91.84	
Kappa Coefficient	0.81		0.84		0.86		0.89	

Accuracy Assessment

Accuracy assessment techniques have been used to evaluate the accuracy of LULC maps produced by random classification methods. The Kappa coefficient value closest to 1 indicates the highest classification accuracy.[53] The overall classification accuracies for 2001, 2011, 2021, and 2024 are 85.50%, 88.50%, 89.00%, and 91.84%, respectively. Correspondingly, the kappa coefficients for these years are 0.81, 0.84, 0.86, and 0.89 (Table 3).

Spatiotemporal Change of LULC in BMC (2001-2024)

The spatiotemporal change in LULC from 2001 to 2024 shows that the only positive change occurred in built-up areas, while green space, wetland, fallow land, and waterbody areas experienced negative changes. Table 4 indicates that built-up areas increased by 5.62% with a growth rate of 16.68%. Fallow land was greatest reduction (-1.87%), and water bodies experienced the highest negative growth rate (-28.98%) from 2001 to 2011. Between 2011 and 2021, built-up areas showed the highest positive growth (15.53%), while waterbodies declined by -24.22%. From 2021 to 2024, fallow land experienced the largest negative growth (-14.94%), whereas built-up areas grew positively by 10.37%. The overall change from 2001-2024 revealed a 16.45% increase in area, with built-up areas showing the highest positive growth rate of 48.78%. Meanwhile, wetlands decreased by -5.19%, waterbodies by -49.04%, followed by fallow land (-30.82%) and greenspace (-20.54%) (Table 4).

Table 4: Change Detection of LULC Area and Growth Rate (%) (2001-2024)

LULC Classes	2001-2011			2011-2021			2021-2024			2001-2024		
	Area in km²	Growth rate (%)	% of area	Area in km²	Growth rate (%)	% of area	Area in km²	Growth rate (%)	% of area	Area in km²	Growth rate (%)	% of area
Built-up area	3.22	16.68	5.62	3.50	15.53	6.11	2.70	10.37	4.72	9.42	48.78	16.45
Wetland	-0.74	-4.99	-1.29	-1.16	-8.24	-2.03	-1.07	-8.28	-1.87	-2.97	-20.04	-5.19
Green space	-0.50	-4.11	-0.87	-1.41	-12.08	-2.46	-0.59	-5.75	-1.03	-2.50	-20.54	-4.37
Fallow land	-1.07	-13.68	-1.87	-0.39	-5.78	-0.68	-0.95	-14.94	-1.66	-2.41	-30.82	-4.21
Waterbodies	-0.91	-28.98	-1.59	-0.54	-24.22	-0.94	-0.09	-5.33	-0.16	-1.54	-49.04	-2.69

Land Transformation Matrix of LULC Classes

The matrix was generated using LULC maps to analyse LULC category transitions and identify gains and losses in LULC classes. The matrix displays changes in area for each LULC class, illustrating how land transformed over the decades. Table 5 shows that the built-up area increased significantly from 19.31 km² in 2001 to 22.53 km² in 2011, mainly due to conversions from other LULC classes, including green space, wetland, fallow land, and waterbodies. Between 2001 and 2011, the largest conversion was from water bodies to built-up areas (Fig. 7a). Greenspace decreased (-4.72 km²), followed by wetlands (-3.51 km²), built-up areas (-2.07 km²), fallow land (-1.66 km²), and water bodies (-1.22 km²) in the study region (Table 5 & Fig. 5, 6a).

Table 5: Land Transformation Matrix of LULC Classes (2001-2011)

Classes	Built-up area	Wetland	Greenspace	Fallow land	Waterbody	Total (2001)	Loss (-)
Built-up area	17.24	0.33	1.45	0.12	0.17	19.31	-2.07
Wetland	1.27	11.31	2.01	0.18	0.05	14.82	-3.51
Greenspace	3.09	1.41	7.45	0.19	0.03	12.17	-4.72
Fallow land	0.87	0.29	0.44	6.16	0.06	7.82	-1.66
Waterbody	0.06	0.74	0.32	0.10	1.92	3.14	-1.22
Total (2011)	22.53	14.08	11.67	6.75	2.23	57.26	
Gain (+)	5.29	2.77	4.22	0.59	0.31		

The matrix of land transformation from 2011 to 2021 shows that built-up areas increased by 5.66 km², with 0.45 km² converted from wetlands, 2.96 km² from green spaces, 1.94 km² from fallow land, and 0.31 km² from water bodies. During this period, wetlands, green spaces, and fallow land lost significant area as they were converted to built-up areas (Table 6, Fig. 5 & 6b).

Table 6: Land Transformation Matrix of LULC Classes (2011-2021)

Classes	Built-up area	Wetland	Greenspace	Fallow land	Waterbody	Total (2011)	Loss (-)
Built-up area	20.37	0.48	1.51	0.06	0.11	22.53	-2.16
Wetland	0.45	11.99	0.28	1.26	0.10	14.08	-2.09
Greenspace	2.96	0.07	8.32	0.29	0.03	11.67	-3.35
Fallow land	1.94	0.03	0.12	4.65	0.01	6.75	-2.10
Waterbody	0.31	0.35	0.03	0.10	1.44	2.23	-0.79
Total (2021)	26.03	12.92	10.26	6.36	1.69	57.26	
Gain (+)	5.66	0.93	1.94	1.71	0.25		

Table 7: Land Transformation Matrix of LULC Classes (2021-2024)

Classes	Built-up area	Wetland	Greenspace	Fallow land	Waterbody	Total (2021)	Loss (-)
Built-up area	23.37	1.12	1.08	0.27	0.19	26.03	-2.66
Wetland	1.11	9.67	1.87	0.19	0.08	12.92	-3.25
Greenspace	2.96	0.46	6.25	0.48	0.11	10.26	-4.01
Fallow land	1.17	0.52	0.30	4.35	0.02	6.36	-2.01
Waterbody	0.12	0.08	0.17	0.12	1.20	1.69	-0.49
Total (2024)	28.73	11.85	9.67	5.41	1.60	57.26	
Gain (+)	5.36	2.18	3.42	1.06	0.40		

The conversion of LULC from 2021 to 2024 indicates that wetland (-3.25 km²) and green space (-4.01 km²) lost area due to land conversion to built-up areas. The built-up area gained the most area (5.36 km²). The land transformation map shows that the north eastern part of BMC was changing from another LULC category to built-up areas (Table 7 & Fig. 5, 6c).

Table 8: Land Transformation Matrix of LULC Classes (2001-2024)

Classes	Built-up area	Wetland	Greenspace	Fallow land	Waterbody	Total (2001)	Loss (-)
Built-up area	16.67	1.10	1.08	0.27	0.19	19.31	-2.64
Wetland	4.01	9.55	1.04	0.14	0.08	14.82	-5.27
Greenspace	3.81	0.72	7.05	0.48	0.11	12.17	-5.12
Fallow land	3.12	0.22	0.16	4.30	0.02	7.82	-3.52
Waterbody	1.12	0.26	0.34	0.22	1.20	3.14	-1.94
Total (2024)	28.73	11.85	9.67	5.41	1.60	57.26	
Gain (+)	12.06	2.30	2.62	1.11	0.40		

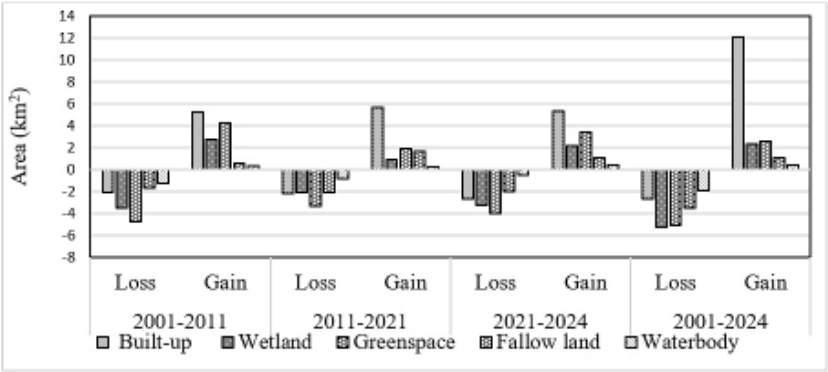

Fig. 5: Area-wise Gain and Loss of LULC Categories (2001-2024)

The final LULC categories transition (2001- 2024) shows significant changes: wetlands (-5.27 km²), green space (-5.12 km²), and fallow land (-3.52 km²) were mainly converted to built-up areas, it increasing about 28.73 km². Built-up areas are mainly in the centre, with green spaces dispersed. The northeastern parts of BMC were growing the built-up areas (Table 8, Fig. 5, 6d).

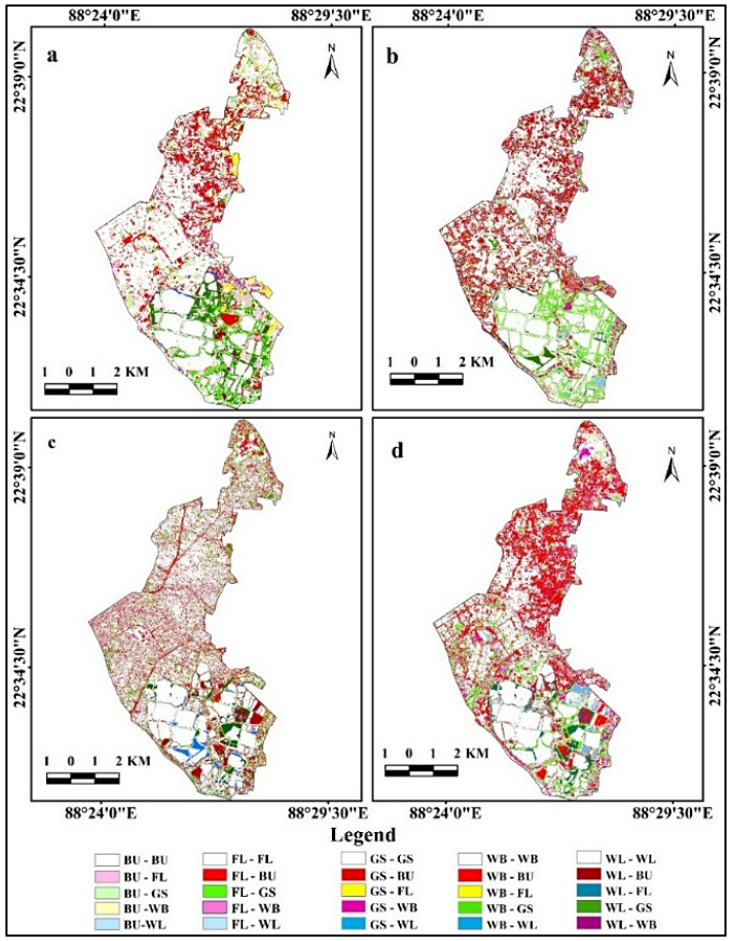

[BU= Built-up, FL= Fallow land, GS= Greenspace, WB= Waterbody, WL= Wetland]
Fig. 6: LULC Classes Conversion Map (a. 2001-2011, b. 2011-2021, c. 2021-2024, d. 2001-2024)

LULC Categories Conversion as Per Chord Diagram (2001-2024)

The Chord diagram visually depicts the transformation of LULC classes in between five categories from 2001 to 2024 through arcs and connecting ribbons. The visualisation effectively reveals dominant shifts, and width of each ribbon indicates the extent of change. In the study area, built-up areas were expanded due to population growth and infrastructure development from 2001 to 2024. The rise of Sector V (NDITA) and New Town as IT and commercial hubs attracted businesses, and migrants, leading to large-scale residential and commercial areas development. The government initiatives also promote real estate projects and accelerate land conversion (Fig. 7).

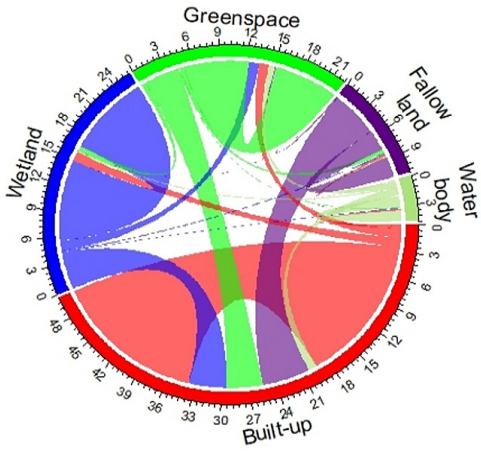

Fig. 7: LULC Categories Conversion Shows Chord Diagram (2001-2024)

Urban Area Expansion Intensity Index (UAEII)

The rate of built-up expansion of the study area has been analysed using the UAEII. The UAEII value is 0.56 for 2001-2011, indicating low urban expansion, and 0.61 for 2011-2021, indicating moderate growth (Table 9). From 2021-2024, the UAEII reached 1.57, clearly signifying high urban growth. Urban area expansion mainly occurs due to infrastructure development, population growth, and the availability of basic amenities. The overall UAEII value (0.72) indicates a moderate pace of urban expansion from 2001-2024, suggesting that the study area is experiencing continuous growth at a stable, controlled rate.

Table 9: Speed of Urban Growth as Per UAEII Growth (2001-11, 2011-21, 2021-24 and 2001-24)

Year	UAEII	Speed of urban growth
2001-2011	0.56	Low
2011-2021	0.61	Medium
2021-2024	1.57	High
2001-2024	0.72	Medium

Identification of Urban Growth using Shannon Entropy

Shannon entropy is used to identify the expansion of urban growth. To analyse the Shannon entropy model, the study area has been divided into five buffer circles with 2 km intervals od built up area of BMC (Fig. 8). Buffer-zone-wise Shannon entropy values have been calculated for 2001, 2011, 2021, and 2024. The entropy value highlights the urban growth of the study area. The entropy values suggest

spatial dispersion of urban growth. The relative entropy for NW from 2001 to 2024 is near the threshold value (Table 10). The absolute entropy values for 2001, 2011, 2021, and 2024 in these zones indicate a compact and planned urban expansion. This growth pattern reflects efficient land utilisation, minimised urban sprawl, and well-organised infrastructure framework, all of which support sustainable urban development and spatial planning.

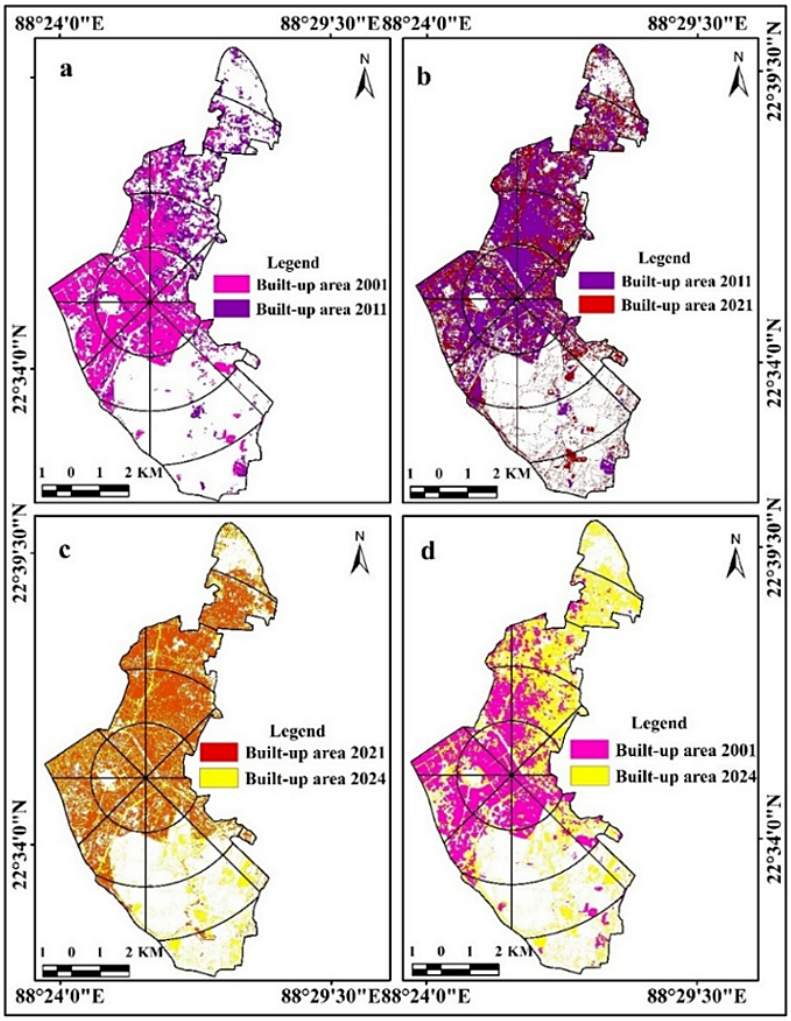

Fig. 8: Spatio-temporal Dynamic of Built-Up Area a) 2001-2011, b) 2011-2021, c) 2021-2024, and d) 2001-2024

Table 10: The Urban Growth as per Shannon Entropy (2001, 2011, 2021 and 2024)

Zones	2001		2011		2021		2024	
	AE	RE	AE	RE	AE	RE	AE	RE
NE	0.152	0.206	0.169	0.217	0.158	0.226	0.164	0.228
SE	0.140	0.221	0.109	0.233	0.099	0.165	0.134	0.224
SW	0.153	0.321	0.161	0.321	0.147	0.307	0.141	0.295
NW	0.154	0.531	0.154	0.511	0.175	0.581	0.152	0.507

(AE= Absolute Entropy, and RE= Relative Entropy)

Modes of Urban Growth

Urban growth is categorised into infilling, edge expansion, and leapfrog growth. It mainly results from infrastructure development driven by increasing population pressure in urban areas. Urban growth occurs through various spatial patterns influenced by population dynamics, economic development, infrastructure expansion, and land-use policies. The modes of urban growth determine how cities expand and change their landscapes over time (Fig. 9). From 2001 to 2011, urban infilling was concentrated within the 2 km to 4 km buffer zone and absent in the 8 km to 10 km zone. This pattern persisted during 2011-2021, with the highest infilling still in the 2 km to 4 km zone, but infilling in the 4 km to 6 km zone declined. In the 6-10 km zone, infilling nearly stopped. Between 2021 and 2024, infilling became irregular and fluctuated across zones, with no clear trend. Meanwhile, edge-expansion growth steadily decreased from the 2 km to 10 km zones (2001-2024), showing less boundary growth as inner-zone consolidation increased. Conversely, leapfrog growth steadily rose, especially farther from the urban core, driven by better connectivity, real estate development, and population pressure.

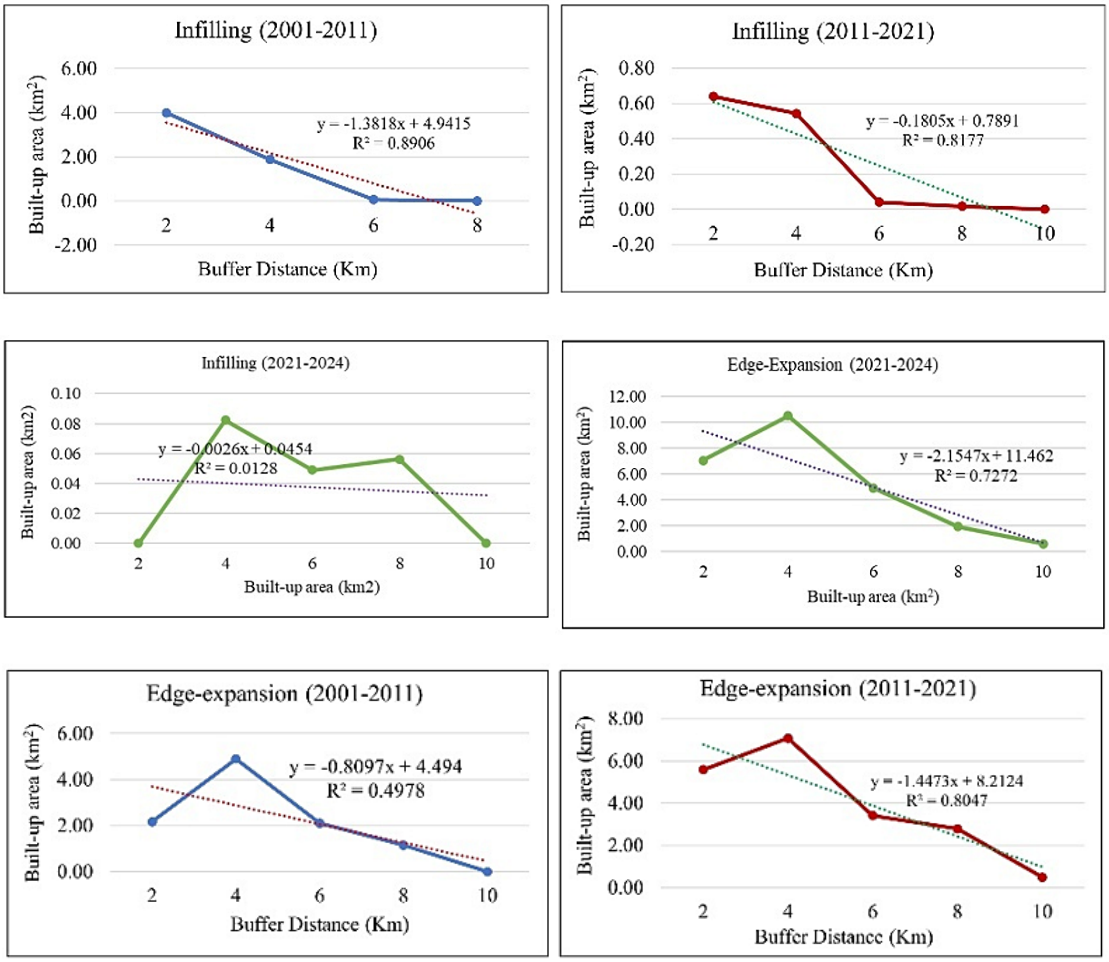

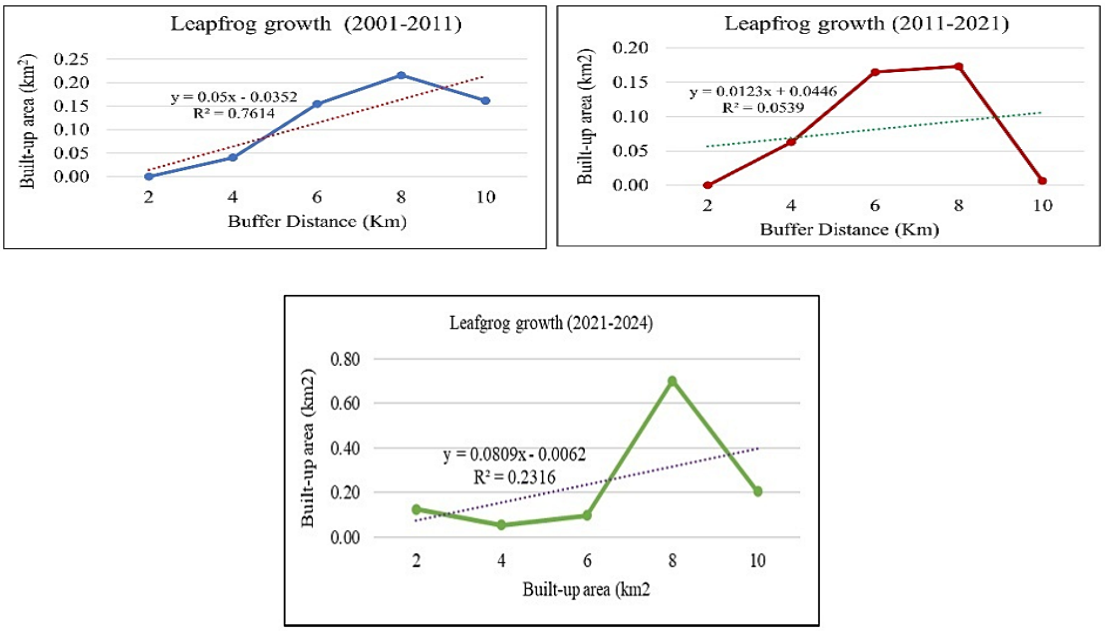

Fig. 9: Modes of Urban Growth

Table 11 illustrates the spatial patterns of urban growth through different modes. Infilling shows a declining trend, while edge expansion rises across the three periods. Meanwhile, leapfrog growth plays a minor role in overall urban expansion. From 2001 to 2011, edge expansion was mainly seen in the northeast, with infilling concentrated in the central area. Leapfrog development occurred in the southeast, driven by the new town in eastern BMC, a planned city in West Bengal. Between 2011 and 2024, some eastern areas experienced intensified edge expansion (Fig. 10). The latest data from 2021 to 2024 indicates a continued decrease in infilling and an increase in edge expansion, suggesting that peripheral areas are experiencing more infrastructure development, while the urban core remains less dense.

Table 11: Modes of Urban Growth (2001-2024)

Modes of urban growth	Urban growth (km²)		
	2001-2011	**2011-2021**	**2021-2024**
Infilling	6.04	1.26	1.19
Edge-expansion	10.47	19.34	23.99
Leapfrog	0.56	0.41	1.18

Discussion

LULC Scenario

The LULC scenarios reveal significant spatial-temporal changes within the study area. Over the years, the BMC area has undergone notable shifts from natural to human-made land cover. These changes are largely influenced by rapid urbanisation, increasing population, and the expansion of transportation networks.[54-56] From 2001 to 2024, the built-up area was the only LULC category to consistently increase an area. This category has shown steady positive growth throughout the study period, indicating ongoing urban expansion driven by population growth, infrastructure development, and economic activity. The ongoing built-up growth reflects the shift from wetlands, green spaces, and

fallow lands into concrete surfaces in the study area. The gradual decline in natural landscapes, such as wetlands and green spaces, poses a potential long-term threat to the environmental and ecological balance of urban environments.[57,58] The persistent depletion of these vital natural resources may lead to adverse effects, including loss of biodiversity, increased urban heat-island effects, reduced air quality, and reduced resilience to climate change.[59-61] Therefore, preserving and integrating natural landscapes into urban planning is crucial to ensuring sustainable, environmentally balanced urban growth.

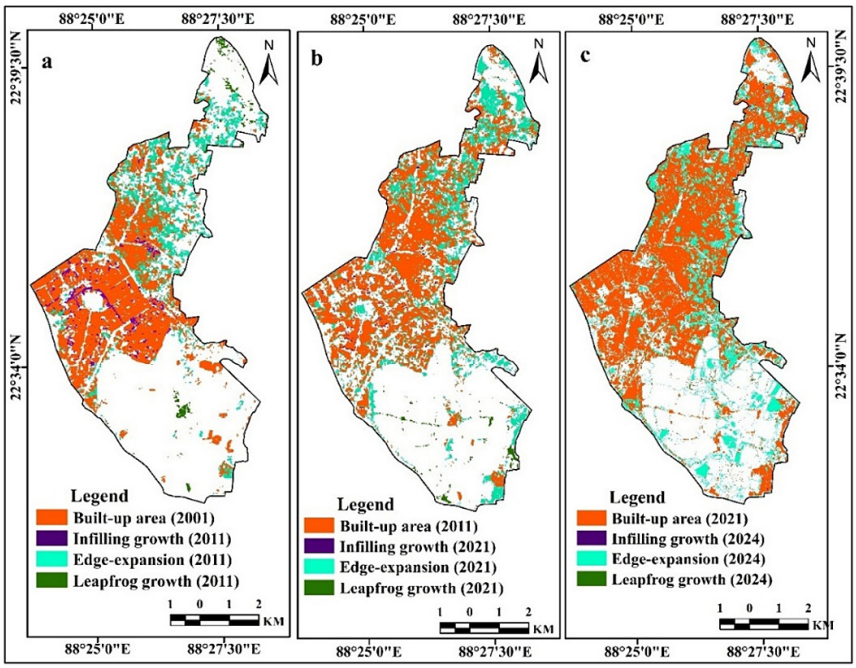

Fig 10: Modes of urban growth a) 2001-2011 b) 2011-2021 c) 2021-2024

Urban Growth Analysis

The infrastructural development within the study region has been analysed from multiple perspectives, focusing on compactness or dispersion, speed, and modes of urban development. Shannon's Entropy Index, the UAEII, and the LEI have been applied to quantify and interpret LULC patterns. These methods collectively provide a comprehensive understanding of urban growth. The UAEII indicates that the study area experienced moderate urban growth between 2001 and 2024. This moderate pace of urban expansion reflects a balanced development process that avoids both rapid growth and stagnation. The Shannon entropy model assessed urban growth in terms of aggregation versus scattering. The results indicate that the overall urban growth pattern reflects a relatively planned and organised development process, and urban development in the study area has generally followed a structured and regulated growth pattern over the analysis period, mainly in the central or core parts of the study area, including sectors I, II, III, IV, and V (Nabadiganta Township). In the Bidhannagar area, the LEI highlights edge expansion as the most prominent, compare to infilling and leapfrog development, primarily due to the availability of undeveloped land along the urban fringes, which facilitates contiguous outward development. The core areas of Bidhannagar are relatively saturated, limiting opportunities for infilling growth, while planning regulations restrict scattered outlying or leapfrog development. The dominance of edge expansion suggests a gradual, continuous extension of the urban fabric rather than isolated developments or densification within the urban core.

Conclusion

Bidhannagar Municipal Corporation, LULC maps were provides a clear view of past and present land-use scenario. The LULC maps indicates an increase of built-up area for residential and commercial

purposes like IT hubs have developed in Sector V, attracting national and international companies and people seeking better opportunities. Further, the most important administrative buildings in Kolkata are located in Bidhannagar. The land transformation matrix also represents the maximum area of wetlands, green spaces, fallow land, and water bodies that are converted into built-up for infrastructural development. For this study also applied UAEII, Shannon entropy, and LEI models. The UAEII values indicates that the study area experienced moderate urban growth from 2001 to 2024. Urban growth is occurring in a compact, planned manner, as ensured by the Shannon entropy values for the zone-wise. The LEI of Bidhannagar reflects that the mode of urban expansion, mainly edge-expansion, covered the maximum area, followed by infilling and leapfrog growth. The findings of the present work provide a valuable approach to decision-making that enables sustainable, eco-friendly development. Final all the models' values are indicated built-up area growing in BMC.

Acknowledgement
The authors would like to express their sincere gratitude to the Bidhannagar Municipal Corporation for providing access to various secondary data and information through their official website.

Funding Sources
The first author extends her gratitude to the University Grants Commission (UGC), New Delhi, for providing the Junior Research Fellowship (No. 210510956799).

Conflict of Interest
The authors do not have any conflict of interest.

Data Availability Statement
The manuscript incorporates all datasets generated or examined throughout this research study.

Ethics Statement
This research did not involve human participants, animal subjects, or any material that requires ethical approval.

Informed Consent Statement
This research has been not involving any human participants, and therefore, consent statement is not required.

Permission to reproduce material from other sources
Not Applicable

Author Contributions
- **Vajana Mondal:** Conceptualisation, Fundamental frameworks, Methodology, and Inter-pretation of results, and Mapping and Layout of all Figures.
- **Manika Mallick**: Conceptualisation, Fundamental frameworks, Methodology, and Interpetation of Results.
- **Moumita Hati:** Conceptualisation, Fundamental frameworks, Methodology, and Interpretation of Results.
- **Debasis Das:** Conceptualisation, Fundamental frameworks, Methodology, and Interpretation of Results.
- **Kausik Panja:** Mapping and Layout of all Figures.
- **Deepa Rai:** Mapping and Layout of all Figures.
- **Atoshi Chakma:** Mapping and Layout of all Figures.
- **Y. V. Krishnaiah:** Supervision for Overall Framing of the Research Work, Field Expertiseand Analysis of Results

References

1. Osman M. A., Abdel-Rahman E. M., Onono J. O., Olaka L. A., Elhag M. M., Adan M., Tonnang H. E. Mapping, intensities and future prediction of land use/land cover dynamics using google earth engine and CA-artificial neural network model. *PLoS One*. 2023; 18(7), e0288694. https://doi.org/10.1371/journal.pone.0288694
2. Kumar S., Ghosh S., Hooda R. S., Singh S. Monitoring and prediction of land use land cover changes and its impact on land surface temperature in the central part of hisar district, Haryana under semi-arid zone of India. *Journal of Landscape Ecology.* 2019;

12(3): 117-140. http://dx.doi.org/10.2478/jlecol-2019-0020

3. Manika M., Krishnaiah Y. V. Spatio-Temporal Detection of Land Use Land Cover Changes in Jalpaiguri District; Geospatial Analysis. *International Journal of Science and Research (IJSR).*2023; 12(2). https://dx.doi.org/10.21275/SR231227231047
4. Lakshiminarayana S., Krishnaiah Y. V. Urban Environmental Problems of Anantapur Municipal Corporation, Andhra Pradesh, India. *Journal of Applicable Chemistry.*2012a; 1(2): 182-195. ISSN 2278-1862 https://www.researchgate.net/publication/267780833_Urban_Environmental_Problems_of_Anantapur_Municipal_Corporation_Andhra_Pradesh_India#fullTextFileContent
5. Wang S W., Munkhnasan L., Lee W. K. Land use and land cover change detection and prediction in Bhutan's high altitude city of Thimphu, using cellular automata and Markov chain. *Environmental Challenges.* 2021; 2, 100017. https://doi.org/10.1016/j.envc.2020.100017
6. Xie, Y., Hunter, M., Sorensen, A. US farmland under threat of urbanization: Future development scenarios to 2040. *Land.* 2023; 12(3): 574. https://doi.org/10.3390/land12030574
7. Alqadhi S., Mallick J., Balha A. Spatial and decadal prediction of land use/land cover using multi-layer perceptron-neural network (MLP-NN) algorithm for a semi-arid region of Asir, Saudi Arabia. *Earth Science Informatics.* 2021; 14: 1547-1562. https://doi.org/10.1007/s12145-021-00633-2
8. Jongkor T., Krishnaiah Y. V., Longkumer L. A. Comparative Study of Urban Infrastructure Facilities of Kohima, Dimapur, and Mokokchung Towns, Nagaland, India. *International Journal of Global Science Research.* 2023; 10(1): 2029-2051. http://dx.doi.org/10.26540/ijgsr.v10.i1.2023.236
9. Panja K., Krishnaiah Y. V., Chakma A., Mallick M., Rai D., Hati M., Das D. Impact of Rubber Plantation Growth on LULC Changes in Eastern-Himalayan Region of West Tripura District Using Geospatial Approach. *International Journal of Ecology and Environmental Sciences.* 2023; 49(5): 533-548. https://doi.org/10.55863/ijees.2023.2852
10. Hati M., Krishnaiah Y. V., Das D., Mallick M., Mondal V., Panja K., Rai D., Chakma A. Impact of Land Use Land Cover Change on Land Surface Temperature of Paschim Bardhaman District, India. *Current World Environment.* 2025a; 20(1). http://dx.doi.org/10.12944/CWE.20.1.24
11. Lukas P., Melesse A. M., Kenea T. T. Prediction of future land use/land cover changes using a coupled CA-ANN model in the upper omo–gibe river basin, Ethiopia. *Remote Sensing.*2023; 15(4): 1148. https://doi.org/10.3390/rs15041148
12. Ahmadlou M., Delavar M R., Basiri A. A comparative study of machine learning techniques to simulate land use changes. *Journal of the Indian Society of Remote Sensing.* 2019; 47: 53-62. https://doi.org/10.1007/s12524-018-0866-z
13. Dinda S., Chatterjee N D., Ghosh S. An integrated simulation approach to the assessment of urban growth pattern and loss in urban green space in Kolkata, India: A GIS-based analysis. *Ecological Indicators.* 2021; 121: 107178. https://doi.org/10.1016/j.ecolind.2020.107178
14. Bardhan M. Monitoring landuse category and landcover change over time through application of RS and GIS – A case study of Salt Lake Town, West Bengal. *Golden Research Thoughts.* 2014; 3(12).
15. Singh S., Karmakar S. Evaluating sustainable urbanization: A comparative study between Salt Lake town and New Town, West Bengal, India. *Journal of Sustainable Science and Transformative Research-Reviews & Letters.* 2023; 2(1): 79-82.
16. Breiman L. Random forests. *Machine learning*. 2001; 45: 5-32.
17. Rimal B., Zhang L., Keshtkar H., Wang N., Lin Y. Monitoring and modeling of spatiotemporal urban expansion and land-use/land-cover change using integrated Markov chain cellular automata model. *ISPRS International Journal of Geo-Information.* 2017; 6(9): 288. https://doi.org/10.3390/ijgi6090288
18. Amini S., Saber M., Rabiei-Dastjerdi H., Homayouni S. Urban land use and land cover change analysis using random forest classification of landsat time series. *Remote Sensing.* 2022; 14(11): 2654. https://doi.

org/10.3390/rs14112654

19. Singh S. K., Mustak S., Srivastava P. K., Szabo S., Islam T. Predicting spatial and decadal LULC changes through cellular automata Markov chain models using earth observation datasets and geo-information. *Environmental Processes.* 2015; 2: 61-78. https://doi.org/10.1007/s40710-015-0062
20. Jamal S., Ali M. B., Ali M. A., Ajmal U. Evaluation and distribution of urban green spaces in Kolkata Municipal Corporation: an approach to urban sustainability. In Towards sustainable natural resources: *monitoring and managing ecosystem biodiversity.* 2022; 151-172. https://link.springer.com/chapter/10.1007/978-3-031-06443-2_9
21. Takada T., Miyamoto A., Hasegawa S. F. Derivation of a yearly transition probability matrix for land-use dynamics and its applications. *Landscape ecology.* 2010; 25: 561-572.
22. Roy S. K., Alam M. T., Mojumder P., Mondal I., Kafy A. A., Dutta M., Ferdous M. N., Al Mamun M. A., Mahtab S. B. Dynamic assessment and prediction of land use alterations influence on ecosystem service value: A pathway to environmental sustainability. *Environmental and sustainability indicators*. 2024; 21: 100319. https://doi.org/10.1016/j.indic.2025.100622
23. Al-Sharif A. A., Pradhan B., Shafri H. Z. M., Mansor S. Quantitative analysis of urban sprawl in Tripoli using Pearson's Chi-Square statistics and urban expansion intensity index. In IOP conference series: *Earth and environmental science.* 2014; 20(1): 012006. https://doi:10.1088/1755-1315/20/1/012006
24. Shannon CE. A Mathematical theory of communication. *Bell Syst Tech J.* 1948; 27(3): 379-423 http://dx.doi.org/10.1002/j.1538-7305.1948.tb01338.x
25. Patra P K., Behera D., Goswami S. Relative shannon's entropy approach for quantifying urban growth using remote sensing and GIS: a case study of Cuttack City, Odisha, India. *Journal of the Indian Society of Remote Sensing.* 2022; 50(4): 747-762. https://doi.org/10.1007/s12524-022-01493-z
26. Zeshan M. T., Mustafa M R U., Baig M. F. Monitoring land use changes and their future prospects using GIS and ANN-CA for Perak River Basin, Malaysia. *Water.* 2012; 13(16): 2286. https://doi.org/10.3390/w13162286
27. Masek J. G., Vermote E. F., Saleous N. E., Wolfe R., Hall F. G., Huemmrich K. F., Gao F., Kutler J., Lim T. K. A Landsat surface reflectance dataset for North America, 1990-2000. *IEEE Geoscience and Remote sensing letters.* 2006; 3(1): 68-72.
28. Vermote E., Justice C., Claverie M., Franch B. Preliminary analysis of the performance of the Landsat 8/OLI land surface reflectance product. *Remote sensing of environment.* 2016; 185: 46-56. http://dx.doi.org/10.1016/j.rse.2016.04.008
29. Nitze I., Barrett B., Cawkwell F. Temporal optimisation of image acquisition for land cover classification with Random Forest and MODIS time-series. *International Journal of Applied Earth Observation and Geoinformation.* 2015; 34: 136-146. https://doi.org/10.1016/j.jag.2014.08.001
30. Pande C. B., Srivastava A., Moharir K. N., Radwan N., Mohd Sidek L., Alshehri F., Pal S. C., Tolche A. D., Zhran M. Characterizing land use/land cover change dynamics by an enhanced random forest machine learning model: a Google Earth Engine implementation. *Environmental Sciences Europe*. 2024; 36(1): 84. https://doi.org/10.1186/s12302-024-00901-0
31. Rodriguez-Galiano V. F., Chica-Olmo M., Abarca-Hernandez F., Atkinson P. M., Jeganathan C. J. R. S. E. Random Forest classification of Mediterranean land cover using multi-seasonal imagery and multi-seasonal texture. *Remote Sensing of Environment.* 2012a; 121: 93-107. https://doi.org/10.1016/j.rse.2011.12.003
32. Rodriguez-Galiano V. F., Ghimire B., Rogan J., Chica-Olmo M., Rigol-Sanchez J. P. An assessment of the effectiveness of a random forest classifier for land-cover classification. *ISPRS journal of photogrammetry and remote sensing.* 2012b; 67: 93-104. http://dx.doi.org/10.1016/j.isprsjprs.2011.11.002
33. Ghosh A., Sharma R., Joshi P.K. Random forest classification of urban landscape using Landsat archive and ancillary data: Combining seasonal maps with decision level fusion. *Applied Geography.* 2014; 48: 31-41. http://dx.doi.org/10.1016/j.apgeog.2014.01.003

34. Adam E., Mutanga O., Odindi J. Land-use/cover classification in a heterogeneous coastal landscape using RapidEye imagery: evaluating the performance of random forest and support vector machines classifiers. *International Journal of Remote Sensing.*2014; 35(10): 3440-3458. https://doi.org/10.1080/01431161.2014.903435
35. Mohibul S., Siddiqui L., Siddiqui M A., Sarif M. M., Parveen N., Islam M.S., Khan S., Khanam N., Shariq M., Nasrin T. Spatio-temporal analysis of land use/land cover change using STAR method in Kolkata Urban agglomeration. In Challenges of Disasters in Asia: *Vulnerability, Adaptation and Resilience.* 2022; 187-207. https://doi.org/10.1007/978-981-19-3567-1_12
36. Van Vliet J., Bregt A K., Hagen-Zanker A. Revisiting Kappa to account for change in the accuracy assessment of land-use change models. *Ecological modelling*. 2011; 222(8): 1367-1375. https://doi.org/10.1016/j.ecolmodel.2011.01.017
37. Huang H., Zhou Y., Qian M., Zeng Z. Land use transition and driving forces in Chinese Loess Plateau: A case study from Pu County, Shanxi Province. *Land.* 2021; 10(1): 67. https://doi.org/10.3390/land10010067
38. Banerjee I., Dutta R. Modelling spatio-temporal pattern of urban sprawl with geospatial techniques: a case of Siliguri city, West Bengal, India. *Letters in Spatial and Resource Sciences.* 2024; 17(1): 23. https://doi.org/10.1007/s12076-024-00386-8
39. Zhang C., Li D. Effect of loading rate on energy and acoustic emission characteristics of tensile fracture and shear fracture for red sandstone. *Theoretical and Applied Fracture Mechanics.* 2024; 104531. https://doi.org/10.1016/j.tafmec.2024.104531
40. Manesha E. P. P., Jayasinghe A., Kalpana H. N. Measuring urban sprawl of small and medium towns using GIS and remote sensing techniques: A case study of Sri Lanka. *The Egyptian Journal of Remote Sensing and Space Science.* 2021; 24(3): 1051-1060. https://doi.org/10.1016/j.ejrs.2021.11.001
41. Barman S., Roy D., Sarkar C. B., Almohamad H., Abdo H. G. Assessment of urban growth in relation to urban sprawl using landscape metrics and Shannon's entropy model in Jalpaiguri urban agglomeration, West Bengal, India. *Geocarto International.* 2024; 39(1): 2306258. https://doi.org/10.1080/10106049.2024.2306258
42. Zachary D., Dobson S. Urban development and complexity: Shannon entropy as a measure of diversity. *Planning Practice & Research.* 2021; 36(2): 157-173. https://doi.org/10.1080/02697459.2020.1852664
43. Das S., Angadi D P. Assessment of urban sprawl using landscape metrics and Shannon's entropy model approach in town level of Barrackpore sub-divisional region, India. *Modeling Earth Systems and Environment.* 2021; 7(2): 1071-1095. https://doi.org/10.1007/s40808-020-00990-9
44. Lakshiminarayana S., Krishnaiah Y. V. Morphological Growth of the Anantapur Town, Andhra Pradesh. *Earth Surface Review.* 2012b; 3(2): 26-32. ISSN 0976-0768 https://www.researchgate.net/publication/299369035_Morphological_Growth_of_the_Anantapur_Town_Andhra_Pradesh#fullTextFileContent
45. Verma S., Chatterjee A., Mandal N. R. Analysing Urban Sprawl and Shifting of Urban Growth Centre of Bengaluru City, India Using Shannon's Entropy Method. *Journal of Settlements & Spatial Planning.* 2017; 8(2). https://doi.org/10.24193/JSSP.2017.2.02
46. Manikandan S. Spatial and temporal dynamics of urban sprawl Using multi-temporal images and relative Shannon entropy model in Adama, Ethiopia. *Journal of Advanced Research in Geo Sciences & Remote Sensing.* 2019; 5(3): 48-57. https://doi.org/10.24321/2455.3190.201801
47. Thomas R W. Information statistics in geography. In: *Concepts and Techniques in Modern Geography, no 31. Geo Abstracts Norwich.* 1981.
48. Sarif M. O., Gupta R. D. Comparative evaluation between Shannon's entropy and spatial metrics in exploring the spatiotemporal dynamics of urban morphology: a case study of Prayagraj City, India (1988–2018). *Spatial Information Research.* 2021; 29(6): 961-979. https://doi.org/10.1007/s41324-021-00406-5
49. Bhatta B. Analysis of urban growth pattern using remote sensing and GIS: a case study of Kolkata, India. *International Journal of*

Remote Sensing. 2009; 30(18): 4733-4746. https://doi.org/10.1080/01431160802651967

50. Chakraborty S., Dadashpoor H., Novotný J., Maity I., Follmann A., Patel P. P., Roy U., Pramanik S. In pursuit of sustainability–Spatio-temporal pathways of urban growth patterns in the world's largest megacities. *Cities.* 2022; 131: 103919. https://doi.org/10.1016/j.cities.2022.103919
51. Liu X., Li X., Chen Y., Tan Z., Li S., Ai B. A new landscape index for quantifying urban expansion using multi-temporal remotely sensed data. *Landscape ecology.* 2010; 25: 671-682.
52. Jiao L., Mao L., Liu Y. Multi-order landscape expansion index: *Characterizing urban expansion dynamics. Landscape and Urban Planning*. 2015; 137: 30-39. https://doi.org/10.1016/j.landurbplan.2014.10.023
53. Singh G., Pandey A. Evaluation of classification algorithms for land use land cover mapping in the snow-fed Alaknanda River Basin of the Northwest Himalayan Region. *Applied Geomatics.* 2021; 13(4): 863-875. https://doi.org/10.1007/s12518-021-00401-3
54. Ray R., Das A., Hasan M. S. U., Aldrees A., Islam S., Khan M. A., Lama G. F. C. Quantitative analysis of land use and land cover dynamics using geoinformatics techniques: A case study on Kolkata metropolitan development authority (KMDA) in West Bengal, India. *Remote Sensing.* 2023; 15(4): 959.
55. Demisse Negesse M., Hishe S., Getahun K. LULC dynamics and the effects of urban green spaces in cooling and mitigating micro-climate change and urban heat island effects: a case study in Addis Ababa City, Ethiopia. *Journal of Water and Climate Change.* 2024; 15(7): 3033-3055. https://doi.org/10.2166/wcc.2024.662
56. Hati, M., Krishnaiah, Y. V., Das, D., Mallick M., Mondal V., Panja K., Chakma A. Assessment of Thermal Comfort and Heat Risk in Predominant Urban Heat Islands of Paschim Bardhaman District, West Bengal, India. *International Journal of Ecology and Environmental Sciences.* 2025; 51(4): 449-470. https://doi.org/10.55863/ijees.2025.0707
57. Krishnaiah, Y.V. Landuse Pattern and Landuse Efficiency of the Papagni river basin, India. *The Indian Journal of Spatial Science.* 2013; 4 (1), 59-68. (www.indiansss.org) https://www.researchgate.net/publication/299368862_Landuse_Pattern_and_Landuse_Efficiency_ of_the_Papagni_River_Basin_India#fullTextFileContent
58. Rana Bora and Krishnaiah, Y.V. Spatial distribution of landuse concentration and landuse efficiency of the Kakodonga river basin, Assam. *National Geographical Journal of India*. 2021; 67 (3), 282-293. https://doi.org/10.48008/ngji.1777 https://www.researchgate.net/publication/355319406_Spatial_distribution_of_land_use_concentration_and_land-use_efficiency_of_the_Kakodonga_river_basin_Assam
59. Tinurenla Jongkor, Krishnaiah, Y. V., Lanusashi Longkumer. Urban Problems of Kohima, Dimapur, and Mokokchung Towns of Nagaland, India. *International Journal of Global Science Research.* 2023; 10 (1), 2029-2051. http://dx.doi.org/10.26540/ijgsr.v10.i1.2023.236
60. Panja K, Krishnaiah Y V, Das D, Hati M, Mondal V, Chakma A. Land capability assessment for land use planning in West Tripura District, Northeast India: An integrated AHP-MCDA approach. *Asian J. Agric.* 2026; 10 (1): g100114. https://doi.org/10.13057/asianjagric/g100114
61. Samel Debbarma, Krishnaiah Y V., Manika Mallick, Moumita Hati, Debasis Das, Vajana Mondal. Evaluation of Land Capability and Sustainable Agricultural Suitability in Khowai District, Tripura, India: An Integration of RS, GIS & AHP Approaches, *International Journal of Plant and Environment.* 2025; 11(3), 536-546. DOI:10.18811/ijpen.v11i03.11 https://www.ijplantenviro.com/index.php/IJPE/article/view/2404/1122